Proceedings of the 2012 IFAC Workshop on Automatic Control in Offshore Oil and Gas Production, Norwegian University of Science and Technology, Trondheim, Norway, May 31 - June 1, 2012

Motion Planning and Tracking of Subsea Structures

Eugenio Fortaleza *

* *Departamento de Engenharia Mecanica, Faculdade de Tecnologia, Universidadde de Brasilia,ZIP Code 70910-900 Brasilia - Brazil (e-mail: efortaleza@unb.br).*

Abstract: This article uses an active control dedicated to the positioning of subsea structures like flow lines. This kind of operation consists in connecting the bottom end of a very long pipeline to the wellhead, by dynamically modifying the pipeline top end position, which is linked to a Dynamically Positioned Vessel (DPV). Such long pipelines are usually called risers, because they are used to rise the drilling mud or the hydrocarbons from the wellhead to the platform. Nowadays this operation is often done manually. The use of an active control intends to reduce the operation time, and to make it possible even under bad weather conditions. The considered subsea structure can be aproximated as a cable submerged in a flow and modelled by the Bernoulli cable equation, completed with a damping factor, that linearly depends on the structure speed. This article tests previous works regarding the tracking system used to follow the reference trajectory of the motion planning considering the Euler-Bernoulli beam equation for large rotations, that is the most used model to define the dynamic behavior of this kind of structures.

Keywords: Offshore structures, Active Control, Motion Planning, Tracking.

1. INTRODUCTION

Deeper and deeper, subsea drilling and exploration represent new technological challenges for the offshore oil industry. One of these challenges is the installation of longer and longer structures to link the oil platform to the seabed.

The reentry operation consists in positioning the riser bottom end above the wellhead in order to connect them while controlling the riser bottom end by the displacements of the surface vessel, in spite of the riser's flexibility, of waves and subsea currents. To reach this goal, it is necessary to move the riser bottom end to the wellhead as fast as possible and to make it stop accurately above the wellhead. The main idea is, first, to design an open loop trajectory to move the riser bottom end from its initial position to the wellhead and, second, a closed loop controller to ensure that the bottom end position prescribed trajectory is satisfactorily tracked in presence of various types of unknown disturbances. This work tests the control system proposed by Fortaleza et al. Fortaleza et al. (2008) and Fortaleza et al. (2011) considering the Euler-Bernoulli beam equation for large rotations, that is the most used equation to define the dynamic behavior of this kind of structures.

2. GOVERNING EQUATIONS

Equation (1) is the Euler-Bernoulli for a beam under traction and external forces from the fluid, It is the most used equation to represent subsea structures like risers and mooring cables. z represents the vertical direction,

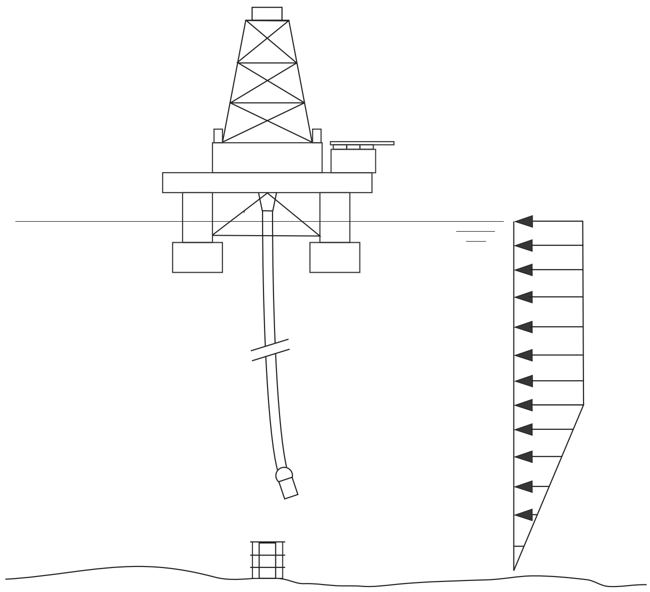

Fig. 1. Platform during the reentry operation

m_s the riser linear mass, E the Young's modulus, Υ the horizontal displacement of the structure and t the time.

$$m_s \frac{\partial^2 \Upsilon}{\partial t^2} = -\frac{\partial^2 \Upsilon}{\partial z^2}\left(EJ\frac{\partial^2 \Upsilon}{\partial z^2}\right) + \frac{\partial}{\partial z}\left(T(z)\frac{\partial \Upsilon}{\partial z}\right) + F_n(z,t) \tag{1}$$

Subsea structures usually have uniform cross-section, in these cases the equation (1) can be represented by:

$$m_s \frac{\partial^2 \Upsilon}{\partial t^2} = -EJ\frac{\partial^4 \Upsilon}{\partial z^4} - \frac{3EA}{2}\left(\frac{\partial \Upsilon}{\partial z}\right)^2\left(\frac{\partial^2 \Upsilon}{\partial z^2}\right) + \frac{\partial}{\partial z}\left(T(z)\frac{\partial \Upsilon}{\partial z}\right) + F_n(z,t) \tag{2}$$

In these cases, the transversal force associated to the beam model is represented by Euler-Bernoulli beam equation for large rotations. The transversal force associated to the traction is similar to the internal transversal force in a cable, and is represented by $\partial(T(z)(\partial\Upsilon/\partial z))/\partial z$. In some special cases, the difference between these two terms is so large that the structure behavior can be represented by only one of them. This is often the case for flexible risers, that are usually slender with small second moment of area J when compared to the riser length ($J = \pi r^4/4$ for a circular section of radius r).

2.1 Hydrodynamic forces

The hydrodynamic forces are defined in a general way by the Navier-Stokes equations. They are the unique external forces, except for the riser structure ends where external forces are present due to the boundary conditions. In the case of the reentry operation, the main hydrodynamic forces are in the plane including the riser bottom end and the wellhead. These forces denoted $F_n(z,t)$ can be defined by the Morison's equation (valid for the actual Reynolds number of the flow around the structure):

$$F_n(z,t) = -m_F\frac{\partial^2 \Upsilon}{\partial t^2} - \mu\frac{\partial \Upsilon}{\partial t}\left|\frac{\partial \Upsilon}{\partial t}\right| \tag{3}$$

In this equation, μ is the drag constant and m_F is the fluid added mass. Denoting $m = m_S + m_F$, and considering the hydrodynamic force (3), equation (2) becomes

$$m\frac{\partial^2 \Upsilon}{\partial t^2} = -EJ\frac{\partial^4 \Upsilon}{\partial z^4} - \frac{3EA}{2}\left(\frac{\partial \Upsilon}{\partial z}\right)^2\left(\frac{\partial^2 \Upsilon}{\partial z^2}\right) + \frac{\partial}{\partial z}\left(T(z)\frac{\partial \Upsilon}{\partial z}\right) - \mu\frac{\partial \Upsilon}{\partial t}\left|\frac{\partial \Upsilon}{\partial t}\right| \tag{4}$$

In practical cases, the displacement has low frequencies, the beam effects can be neglected. The tension for a disconnected riser in these conditions is a linear function of its weight ($T = (m_s - \rho S)z$), where ρ represents the water density and S the transverse section surface. Neglecting the beam effects and dividing equation (4) by m we get:

$$\frac{\partial^2 \Upsilon}{\partial t^2} = +\frac{\partial}{\partial z}\left(\frac{(m_s-\rho S)z}{m}\frac{\partial \Upsilon}{\partial z}\right) - \frac{\mu}{m}\frac{\partial \Upsilon}{\partial t}\left|\frac{\partial \Upsilon}{\partial t}\right| \tag{5}$$

The constant term $(m_s - \rho S)/m$ can be replaced by an effective gravity g. It is proposed to linearize the drag term, substituting the term $\frac{\mu}{m}|\frac{\partial \Upsilon}{\partial t}|$ by the constant τ, that is calculated as a function of μ/m and of the mean value of $\frac{\partial \Upsilon}{\partial t}$ along the structure. With this approximation the system equation becomes the cable equation defined by Bernoulli (see Petit and Rouchon (2001)) plus a linear damping factor:

$$\frac{\partial^2 \Upsilon}{\partial t^2}(z,t) = \frac{\partial}{\partial z}\left(gz\frac{\partial \Upsilon}{\partial z}(z,t)\right) - \tau\frac{\partial \Upsilon}{\partial t}(z,t) \tag{6}$$

3. A USEFUL FORMULA

This section presents an analytical solution of equation (6) in the Laplace domain, following the idea proposed by Petit and Rouchon Petit and Rouchon (2001) for an undamped cable and here adapted to a damped cable. This solution is useful to define the behavior of the riser bottom end as function of the riser top position with out the imprecisions due to the space discretization. This solution is used to calculate the motion planning, and the tracking system of section 6. The first step is the change of variable $l = 2\sqrt{z/g}$, which yields $\frac{\partial}{\partial z} = \frac{2}{gl}\frac{\partial}{\partial l}$, transforming equation (6) into a $g-$independent equation:

$$-l\frac{\partial^2 \Upsilon}{\partial t^2}(l,t) - \tau l\frac{\partial \Upsilon}{\partial t}(l,t) + \frac{\partial \Upsilon}{\partial l}(l,t) + l\frac{\partial^2 \Upsilon}{\partial l^2}(l,t) = 0 \tag{7}$$

Using a $t-$Laplace transform and considering the cable at rest at $t = 0$, equation (7) can be rewritten, with $\widehat{\Upsilon}$ the Laplace transform of Υ, as the following ordinary differential equation:

$$-ls^2\widehat{\Upsilon}(l,s) - \tau ls\widehat{\Upsilon}(l,s) + \frac{\partial \widehat{\Upsilon}}{\partial l}(l,s) + l\frac{\partial^2 \widehat{\Upsilon}}{\partial l^2}(l,s) = 0 \tag{8}$$

The change of variable $\zeta = il\sqrt{s(s+\tau)}$ transforms (8) into a Bessel equation of the first kind:

$$\zeta\widehat{\Upsilon}(\zeta,s) + \frac{\partial \widehat{\Upsilon}}{\partial \zeta}(\zeta,s) + \zeta\frac{\partial^2 \widehat{\Upsilon}}{\partial \zeta^2}(\zeta,s) = 0 \tag{9}$$

Its solution $\widehat{\Upsilon}(z,s)$ has the following form:

$$\widehat{\Upsilon}(z,s) = c_1 J_0(2i\sqrt{s(s+\tau)}\sqrt{z/g}) + c_2 Y_0(2i\sqrt{s(s+\tau)}\sqrt{z/g}) \tag{10}$$

Here J_0 and Y_0 are respectively the Bessel functions of first and second kinds (see Abramowitz and Stegun (1972)). Sought after solutions being finite for $\zeta = 0$, they are such that $c_2 = 0$:

$$\widehat{\Upsilon}(z,s) = \widehat{\Upsilon}(0,s)J_0(2i\sqrt{s(s+\tau)}\sqrt{z/g}) \tag{11}$$

4. MOTION PLANNING

This solution, namely (11), proves that the corresponding model turns out to be differentially flat, because any state of the system and its input (position and speed of the structure along the z-axis) can be calculated from the bottom trajectory (flat output), see Fliess et al. (1995) and Lévine (2009) for more details. This useful property is now used to design the motion planning. The solution (11), is now expanded in Taylor's series, in order to formally invert the Laplace transform. Then we deduce, in the time domain, an approximation of the open loop riser top end trajectory, that is a function of the reference trajectory for the riser bottom end.

We rewrite equation (11) using J_0's integral formula (see e.g. Abramowitz and Stegun (1972)):

$$\widehat{\Upsilon}(z,s) = \frac{1}{2\pi}\int_{-\pi}^{\pi}\exp(-2\sqrt{s(s+\tau)}\sqrt{z/g}\sin\theta)\widehat{\Upsilon}(0,s)d\theta \tag{12}$$

and expand the term $\exp(-2\sqrt{s(s+\tau)}\sqrt{z/g}\sin\theta)$ in equation (12) around $\tau = 0$:

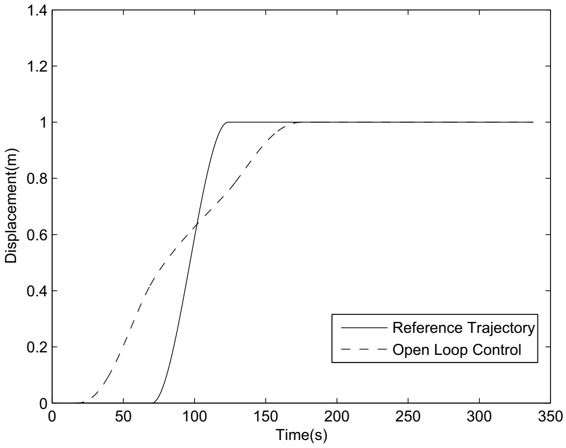

Fig. 2. Open loop control and reference trajectory.

$$
\begin{aligned}
\exp\Big(-2\sqrt{s(s+\tau)}\sqrt{\frac{z}{g}}\sin\theta\Big) &= \exp(-2\sqrt{s^2}\sqrt{z/g}\sin\theta) \\
&+\tau\left(\frac{\partial(\exp(-2\sqrt{s(s+\tau)}\sqrt{z/g}\sin\theta))}{\partial\tau}\right)_{\tau=0} \\
&+\frac{\tau^2}{2}\left(\frac{\partial^2(\exp(-2\sqrt{s(s+\tau)}\sqrt{z/g}\sin\theta))}{\partial\tau^2}\right)_{\tau=0} \\
&+\cdots
\end{aligned}
\tag{13}
$$

Thus

$$
\begin{aligned}
\exp\,(-2\sqrt{s(s+\tau)}\sqrt{z/g}\sin\theta) &= \exp(-2\sqrt{s^2}\sqrt{z/g}\sin\theta) \\
&\left(1-\tau\sqrt{\frac{z}{g}}\sin\theta+\frac{\tau^2}{2}\left(\frac{z\sin^2\theta}{g}+\sqrt{\frac{z}{g}}\frac{\sin\theta}{2s}\right)\right) \\
&+\cdots
\end{aligned}
\tag{14}
$$

and

$$
\begin{aligned}
\Upsilon\,(z,t) = \frac{1}{2\pi}\int_{-\pi}^{\pi}&\left(\Upsilon(0,t-2\sqrt{\frac{z}{g}}\sin\theta)\right. \\
&(1-\tau\sqrt{\frac{z}{g}}\sin\theta+\frac{\tau^2}{2}\frac{z\sin^2\theta}{g}) \\
&\left.+\frac{\tau^2}{4}\int_0^t\Upsilon(0,\varrho-2\sqrt{\frac{z}{g}}\sin\theta)\sqrt{\frac{z}{g}}\sin\theta\, d\varrho+\cdots\right)d\theta
\end{aligned}
\tag{15}
$$

The open loop solution $\Upsilon_o(L,t)$, where L is the riser length, is obtained by numerical integration of (15). The simulation example in Figure 2 shows that the approximations made have a negligible effect on the system response. The considered discrete system in all numerical simulations is obtained by discretizing equation (2). In figure 2, the numerical simulation uses the hydrodynamic force represented in equation (3).

5. LYAPUNOV DESIGN

This section presents a strategy that uses a Lyapunov function to design a tracking system, in order to ensure the stability and reduce the difference between the real position of the structure and its reference trajectory.

Consider the relative displacement Υ_R around the reference trajectory Υ_o: $\Upsilon_R = \Upsilon - \Upsilon_o$. The objective is to define a tracking system to enforce the convergence of Υ_R to zero.

Theorem 1. Consider system (6). The control law

$$
\begin{aligned}
\Upsilon(L,t) &= \Upsilon_o(L,t) \\
&-k\int_0^t\left(g\frac{\partial\Upsilon_R}{\partial z}(L,v)+\frac{\Upsilon_R(L,v)}{\vartheta^2}\right)dv
\end{aligned}
\tag{16}
$$

can be used to asymptotically track any bottom end reference $\Upsilon_o(0,t)$. In equation (16), k is the controller gain, ϑ a tuning parameter, and $\Upsilon_o(L,t)$ a top end reference trajectory, computed from the specified bottom end reference trajectory $\Upsilon_o(0,t)$ from equation (15).

Proof. Consider the system given by (6). Following the idea proposed by Thull et al Thull et al. (2006), a candidate Lyapunov function H, based on the system energy associated to Υ_R, is given by

$$
H = \frac{L\Upsilon_R^2(L,t)}{2\vartheta^2}+\frac{1}{2}\int_0^L\left(z\left(\frac{\partial\Upsilon_R}{\partial z}\right)^2+\left(\frac{\partial\Upsilon_R}{\partial t}\right)^2\right)dz
\tag{17}
$$

Parameter ϑ represents the convergence time and determines the energy associated to the relative displacement of the structure top end. Using equation (6), the time derivative of H is computed as follows:

$$
\begin{aligned}
\frac{dH}{dt} &= \frac{L\Upsilon_R(L,t)}{\vartheta^2}\frac{\partial\Upsilon_R}{\partial t}(L,t)+\int_0^L\left(z\frac{\partial\Upsilon_R}{\partial z}\frac{\partial^2\Upsilon_R}{\partial z\partial t}\right)dz \\
&+\int_0^L\left(\frac{\partial\Upsilon_R}{\partial t}\left(\frac{\partial}{\partial z}\left(gz\frac{\partial\Upsilon_R}{\partial z}\right)-\tau\frac{\partial\Upsilon_R}{\partial t}\right)\right)dz
\end{aligned}
\tag{18}
$$

After integration by parts, we get

$$
\begin{aligned}
\frac{dH}{dt} &= L\frac{\partial\Upsilon_R}{\partial t}(L,t)\left(g\frac{\partial\Upsilon_R}{\partial z}(L,t)+\frac{\Upsilon_R(L,t)}{\vartheta^2}\right) \\
&-\tau\int_0^L\left(\frac{\partial\Upsilon_R}{\partial t}\right)^2dz
\end{aligned}
\tag{19}
$$

We therefore introduce the control law

$$
\frac{\partial\Upsilon_R}{\partial t}(L,t) = -k\left(g\frac{\partial\Upsilon_R}{\partial z}(L,t)+\frac{\Upsilon_R(L,t)}{\vartheta^2}\right)
\tag{20}
$$

With this law, $dH/dt \le 0$, so the system converges to the largest invariant set contained in $dH/dt = 0$.

$$
\begin{aligned}
dH/dt &= -kL\left(g\frac{\partial\Upsilon_R}{\partial z}(L,t)+\frac{\Upsilon_R(L,t)}{\vartheta^2}\right)^2 \\
&-\tau\int_0^L\left(\frac{\partial\Upsilon_R}{\partial t}\right)^2dz
\end{aligned}
\tag{21}
$$

This set is such that

$$
\int_0^L\left(\frac{\partial\Upsilon_R}{\partial t}\right)^2dz = 0
\tag{22a}
$$

$$
\frac{\partial}{\partial z}\left(gz\frac{\partial\Upsilon_R}{\partial z}\right) = 0
\tag{22b}
$$

This first relation implies $\partial\Upsilon_R/\partial t(z,t) = \partial^2\Upsilon_R/\partial t^2(z,t) = 0$ for all z and all t, The application of this result in equation (6) gives the second relation. The solution of the second relation is $\Upsilon_R(z) = c\ln(z)$, where c is an arbitrary

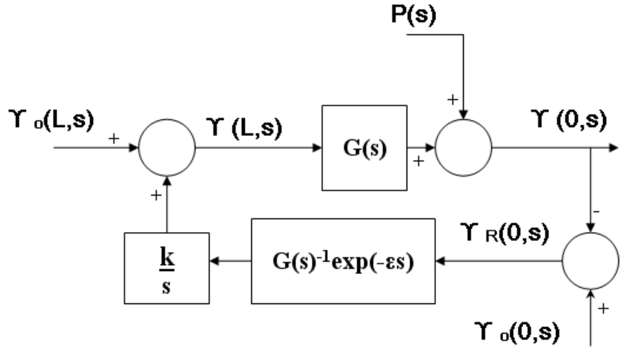

Fig. 3. Block diagram of the tracking system.

constant. At rest, the balance of the external forces is given, at the top end, by the sum of F_t, accounting for the horizontal part of the tension at the top end of the structure, and F_p, the resultant of the disturbances. By definition, F_t is proportional to $\partial\Upsilon_R/\partial z(L,t)$. In this unperturbed case, $F_p = 0$, so $F_t = 0$ and $\partial\Upsilon_R/\partial z(L,t) = 0$, which leads to $\Upsilon_R(L,t) = 0$. The unique possible solution $\Upsilon_R(z) = c\ln(z)$ with $\Upsilon_R(L) = (\partial\Upsilon_R)/(\partial z)(L) = 0$ is $c = 0$. That proves the convergence of Υ_R to zero for all z, and in particular gives $\Upsilon_R(0,t) = \Upsilon_R(L,t) = 0$: the stability is proven.

6. INVERSE MODEL CONTROL

There are different alternatives to attenuate the disturbances. We propose to combine system inversion for tracking, the inverted model being defined by equation (15), with an open loop design that reduces the effect of waves.

Regarding equation (3), it may be seen that an artificial increase of the structure speed $\partial\Upsilon/\partial t$ implies a larger system damping, that reduces the relative effect of the flow speed changes. So, an open loop trajectory, that is fast enough to increase the damping during a given period of time, can reduce the effect of waves. Figure 3 presents the block diagram of the tracking system. The transfer function $G(s)$ between the riser top end $\Upsilon(L,s)$ and the riser bottom end $\Upsilon(0,s)$ is represented by

$$G(s) = \frac{2\pi}{\int_{-\pi}^{\pi} \exp(-2\sqrt{s^2}\sqrt{z/g}\sin\theta)} \tag{23}$$

Theorem 2. Denote Υ_o is the reference trajectoriy and Υ is the real riser position. The control law

$$\begin{aligned}\Upsilon(L,s) = {} & \Upsilon_o(L,s) \\ & -\frac{kG(s)^{-1}e^{-\epsilon s}}{s}(\Upsilon(0,s) - \Upsilon_o(0,s))\end{aligned} \tag{24}$$

stabilizes system (6) around any trajectory $\Upsilon_o(0,s)$ if $k < \pi/(2\epsilon)$.

Proof. The Bessel function of first order J_0 only has real zeros (see e.g. Ismail and Muldoon Ismail and Muldoon (1995)). Thus, the poles of $G(s)$ only lie in the region $Re(s) < 0$. As $G(s)$ does not have unstable zeros or poles, there is no cancellation between unstable zeros and poles in closed loop. The stability of the feedback law can be analyzed by the simplified Nyquist criterion. Denote by $M(s)$ the open loop transfer function between $\Upsilon_o(0,s)$ and $\Upsilon(0,s)$:

$$M(s) = k\exp(-\epsilon s)/s \tag{25}$$

Rewriting $\exp(-\epsilon s)$ in trigonometric form and replacing s by $i\omega$:

$$M(i\omega) = \frac{k(\cos(\epsilon\omega) - i\sin(\epsilon\omega))}{i\omega} \tag{26}$$

For $k > 0$, the largest negative real value of (26) is achieved for $\omega = \omega_0 = \pi/(2\epsilon)$. For this value, $M(\omega_0) = -k/\omega_0$. A sufficient condition for the closed loop stability is $M(\omega_0) > -1$, which leads to $k < \pi/(2\epsilon)$.

In practise, a value of k much smaller than $k < \pi/(2\epsilon)$ is used for the sake of robustness. Typically, $k = \pi/(16\epsilon)$. $G(s)$ has a maximum delay equal to $\epsilon = 2\sqrt{L/g}$ (see equation (15), so its inverse $G(s)^{-1}$ is associated to the same delay to insure causality. The delay of the control estimation is an important problem for the high frequencies, however for the low frequencies this delay is negligible.

Theorem 3. The control law given by equation (24) rejects low frequency disturbances.

Proof. The closed loop transfer function between the disturbance $P(s)$ and the system output $\Upsilon(0,s)$ is

$$\frac{\Upsilon(0,s)}{P(s)} = \frac{s}{s + ke^{-\epsilon s}} \tag{27}$$

Setting $s = i\omega$, the transfer function (27) gives the system gain associated to every frequency ω:

$$\frac{\Upsilon(0,i\omega)}{P(i\omega)} = \frac{i\omega}{i\omega + ke^{-\epsilon i\omega}} \tag{28}$$

For low frequency disturbances ($\omega \to 0$), the influence of the disturbances on the output tends to zero ($|\Upsilon(0,i\omega)/P(i\omega)| \to 0$).

Figure 4 gives an example of what can be obtained with this approach for the control of a structure with waves and sea current disturbances. The tracking system combined to the motion planning stabilizes the riser bottom end at its target during a certain period (region close to $t = 1000$ s in the figure). During this period, the connection of the riser bottom end to the wellhead is possible.

The shape of the reference trajectory is such that the reference speed is kept large enough almost until the end of the displacement to dampen the wave disturbances before the structure has reached its target. It naturally implies that the initial distance between the bottom end of the structure and the wellhead is also large enough

Note, however, that the maximum speed along such reference trajectory cannot be chosen too large for the following reasons:

- if the speed is too large, the small angle assumption may be violated, and higher order terms may be required in the expansion of the damping term;
- if the acceleration is too large, the beam effect may become significant.

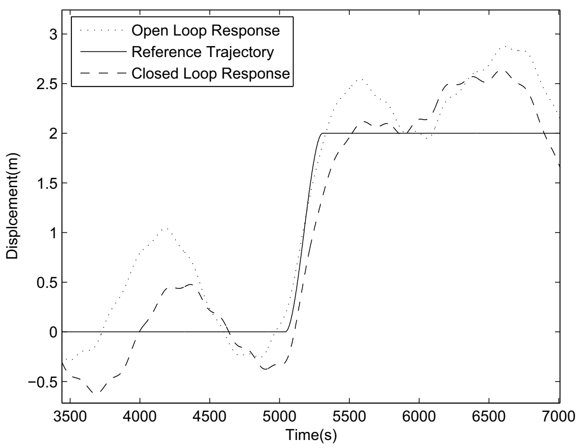

Fig. 4. Structure under disturbances due to wave and sea current effects.

7. CONCLUSION

The motion planning consists in a two steps procedure: first assimilate the structure to a cable with linear damping; then invert the analytical solution to the latter model in the Laplace domain, to express it in the time domain thanks to a series expansion. The final result is a function that has the bottom end as input reference trajectory, and the top end trajectory as output. Without disturbances and model errors, the so-obtained top end trajectory approximately generates the desired bottom end reference trajectory.

Two different closed loop controls have been proposed. The first one is based on a Lyapunov design for which the feedback is based on the top end structure angle measurements. The other way to design a feedback law consists in inverting the previously obtained open loop mapping with the addition of a delay. The main practical result is the possibility of sufficiently attenuating the wave effects to ensure reentry under difficult weather conditions, even when the non linearities due to the beam effect are considered during the numerical simulations.

ACKNOWLEDGMENTS

The author would like to acknowledge the Brazilians institutions: ANP, FINEP, MCT and Petrobras for supporting the present study and the PRH-PB 23.

REFERENCES

Abramowitz, M. and Stegun, I.A. (1972). *Handbook of Mathematical Functions with Formulas, Graphs, and Mathematical Tables.*

Fliess, M., Lévine, J., Martin, P., and Rouchon, P. (1995). Flatness and defect of nonlinear systems: introductory theory and examples. *International Journal of Control*, 61(6), 1327–1361.

Fortaleza, E., Creff, Y., and Levine, J. (2008). Active control and motion planning for offshore structures. *Fourth European Conference on Structural Control, Saint Petersburg*, 1, 226–233.

Fortaleza, E., Creff, Y., and Levine, J. (2011). Active control of a dynamically positioned vessel for the installation of subsea structures. *Mathematical and Computer Modelling of Dynamical Systems*, 17(1), 71–84.

Ismail, M.E.H. and Muldoon, M.E. (1995). Bounds for the small real and purely imaginary zeros of bessel and related functions. *Methods and Applications of Analysis*, 2(1), 1–21.

Lévine, J. (2009). *Analysis and Control of Nonlinear Systems: A Flatness-Based Approach.* Mathematical Engineering Series, Springer.

Petit, N. and Rouchon, P. (2001). Flatness of heavy chain systems. *SIAM Journal on Control and Optimization*, 40, 475–495.

Thull, D., Wild, D., and Kugi, K. (2006). Application of combined flatness- and passivity-based control concept to a crane with heavy chains and payload. *IEEE International Conference on Control Applications*, 656–661.

Appendix A. NUMERICAL SIMULATIONS

The considered discrete system for the numerical simulations in this article comes from the discretization of equation (4). The simulated offshore structure is a typical drilling riser in deep water. Its dimensions and numerical constants are represented in table A.1.

Table A.1. Simulated structure: dimensions and constants.

Type	Value	Unit
Internal Diameter	50	mm
External Diameter	55	mm
Height	2	km
Upper bounder condition	Fixed top	
Lower bounder condition	Free bottom	
Steel Density	7.860×10^3	kg/m^3
Steel Elastic Modulus	210×10^9	Pa
Water Density	10^3	kg/m^3

The numerical model was obtained by finite difference discretization. The continuous function $\Upsilon(z,t)$ was approximated by a discrete vector $Y(t)$ and the derivatives with respect to z by the following recursive formula:

$$\frac{\partial^j Y_n}{\partial z^j} = \frac{1}{l}\left(\frac{\partial^{j-1} Y_{n+0.5}}{\partial z^{j-1}} - \frac{\partial^{j-1} Y_{n-0.5}}{\partial z^{j-1}}\right) \qquad (A.1)$$

The values of Y are only available for $n \in \{0,\ldots,N\}$. Thus, for the first derivatives at $n \in \{0,\ldots,N\}$, since the values $Y_{n+0.5}$ and $Y_{n-0.5}$ are not available, we complete (A.1) by:

$$\frac{\partial Y_n}{\partial z} = \frac{Y_{n+1} - Y_{n-1}}{2l} \qquad (A.2)$$